Available online at www.sciencedirect.com
SCIENCE DIRECT®
Physica B 370 (2005) 46–51
PHYSICA B
www.elsevier.com/locate/physb

Structure and composition of secondary phase particles in cobalt-doped TiO_2 films

B.-S. Jeong[a], Y.W. Heo[a], D.P. Norton[a,*], A.F. Hebard[b]

[a]*Department of Materials Science and Engineering, University of Florida, 100 Rhines Hall, P.O. Box 116400, Gainesville, FL 32611, USA*
[b]*Department of Physics, University of Florida, Gainesville, FL 32611-8440*

Received 6 July 2005; received in revised form 18 July 2005; accepted 19 August 2005

Abstract

The microstructural properties of secondary phase particles formed in epitaxial $Co_xTi_{1-x}O_2$ anatase thin films grown on (0 0 1)$LaAlO_3$ by a reactive RF magnetron co-sputter deposition are examined. These films exhibit ferromagnetic behavior in magnetization measurements, showing a M–H loop at room temperature with a saturation magnetization on the order of 0.7 μ_B /Co. X-ray photoemission spectrometry indicates that the Co cations are in the Co^{2+} valence state. Cross-section electron microscopy reveals that a significant fraction of the cobalt segregates into Co–Ti–O secondary phase particles. Selected area electron diffraction shows that the secondary phase particles are cobalt-rich anatase. While the cobalt is concentrated in the segregated particles, local energy dispersive spectrometry indicates some Co throughout the film.

PACS: 72.25.Dc; 81.15.Cd

Keywords: Sputtering; Semiconductor; Magnetic properties; Microstructure

1. Introduction

In recent years, there has emerged considerable interest in the development of electronics based on the spin of electrons. One approach to realizing novel spin-based electronic devices involves the exploitation of spin-polarized electron distributions in dilute magnetic semiconductor (DMS) materials. In most semiconductors doped with transition metals, the magnetic behavior, if any, is observed at temperatures well below room temperature [1–4]. Among the conventional semiconductors, (Ga, Mn)As exhibits the highest Curie temperature (T_c), on the order of 110 K [5,6]. In recent years, it has been reported that cobalt-doped semiconducting anatase (TiO_2) is ferromagnetic at room temperature [7]. This may provide for the development of spin-based DMS electronics that operate at room temperature if the

*Corresponding author.
E-mail address: dnort@mse.ufl.edu (D.P. Norton).

0921-4526/$ - see front matter © 2005 Elsevier B.V. All rights reserved.
doi:10.1016/j.physb.2005.08.036

ferromagnetic spin moments are present in the free electron distribution.

Ferromagnetic thin films of $Co_xTi_{1-x}O_2$, epitaxially stabilized in the anatase structure, have previously been realized on $SrTiO_3(0\,0\,1)$ and $LaAlO_3(0\,0\,1)$ by pulsed laser deposition (PLD), oxygen plasma-assisted molecular-beam epitaxy (OPA-MBE), and reactive sputter deposition [7–13]. In films grown by each technique, secondary phase Co–Ti–O particles have been reported. The ferromagnetic properties appear to originate from Co substitution on the Ti site in some films, from cobalt metal precipitates in others. From diffraction studies, nanoparticles in a continuous anatase matrix have been observed that are crystalline rutile, anatase, or metallic cobalt [10–12]. For films grown by MBE, the spontaneous magnetic moment per Co atom derived from the saturated magnetization was $0.6\,\mu_B$. This value is 2 times higher than that reported for films deposited by pulsed-laser deposition [7]. Spectroscopic studies on the MBE-grown TiO_2 thin films suggests that the cobalt exists in the Co^{2+} oxidation which is consistent with ferromagnetism originating from Co substitution on the Ti site. However, studies of Co-doped TiO_2 films deposited by pulsed laser deposition suggest that the formation of Co nanoclusters may be responsible for the ferromagnetic properties [8]. For pulsed-laser deposited material, Shinde et al. [11] reported clusters across the entire surface of the films that showed a Co signal only with no oxygen or titanium peaks. Previously, we reported on the transport and magnetic properties of undoped and cobalt-doped semiconducting transparent anatase TiO_2 thin films epitaxially grown by reactive sputtering deposition employing water vapor [13,14]. The cobalt-doped films were shown to be ferromagnetic, but with segregated oxide precipitates. It remains an open question as to the origin of ferromagnetism in these materials, as well as the probable role that the specific processing technique plays in yielding these results.

In this paper, the crystalline structure and composition of the secondary phase particles for Co-doped TiO_2 ($Co_xTi_{1-x}O_2$) epitaxial thin films grown by reactive co-sputter deposition are examined.

2. Experimental procedures

$Co_xTi_{1-x}O_2$ anatase films were epitaxially grown by reactive RF magnetron co-sputter deposition with cation sputtering targets of Ti (99.995%) and Co(99.95%). Water vapor (H_2O) was employed as the oxidant to facilitate the formation of carriers via the creation of oxygen vacancies. The total pressure during growth was fixed at 15 mTorr, whereas the water vapor pressure was varied from 10^{-4} and 10^{-2} Torr. A water vapor pressure of $P(H_2O) = 10^{-3}$ Torr was found to be optimal in realizing oxygen deficiency and semiconductor transport behavior. A substrate temperature during the deposition of 650°C resulted in the growth of highly crystalline epitaxial Co-doped TiO_2 thin films in the anatase phase. The growth rate was on the order of 2 nm/min.

The macroscopic crystalline structure of the Co-doped TiO_2 films was characterized by X-ray diffraction (XRD) with a Cu Kα radiation source. Quantitative analysis of chemical composition was performed by electron probe microanalysis (EPMA). In order to extract information regarding chemical states of the element, X-ray photoelectron spectroscopy (XPS) has been used with Al-Kα radiation ($h\nu = 1486.6$ eV). Surface morphology and chemical mapping were examined by field emission scanning electron microscopy (FESEM) and transmission electron microscopy (TEM) equipped with energy dispersive spectrometry. Room temperature magnetization was measured by a quantum design superconducting quantum interference device (SQUID) magnetometer. The film and secondary particle microstructure and crystal structure was determined with a JEOL 2010 transmission electron microscopy and selected area electron diffraction.

3. Results and discussion

Cobalt-doped epitaxial anatase films deposited at a growth temperature of 650 °C and water vapor pressure at 10^{-3} Torr exhibited crystalline quality similar to that seen in previous work on undoped films. The films are near single phase epitaxial

anatase with a small amount of secondary rutile phase evident in the diffraction data. From in-plane and out-of-plane X-ray diffraction measurement, the anatase lattice parameters were $a = 3.790$ Å and $c = 9.495$ Å. Typical magnetization properties for the Co-doped films are shown via the M–H plots shown in Fig. 1. For the Co-doped TiO_2 samples, hysteresis loops are observed at room temperature for film grown at 650 °C with water vapor as an oxidant. Both the total magnetization and calculated magnetization per Co cation are plotted. These results are consistent with both the MBE and PLD results reported elsewhere [7,9]. The magnetic moment was relatively low (0.25 μ_B per Co ion) at saturation. XPS results are consistent with the Co existing in the +2 formal oxidation state. Backscattered electron images obtained by FESEM and Auger electron spectroscopy show that the sample surface is decorated with segregated nanoclusters. The results are reported elsewhere [13]. Results from AES indicate that the Co dopant is principally located in the segregated areas, with significantly less Co located in the film region between the nanoclusters.

In order to investigate the crystal structure of the segregated nanoclusters, high-resolution transmission electron microscopy (HRTEM) was used. Cross-section TEM images for a 7 at% Co-doped TiO_2 film are shown in Figs. 2 and 3. Several segregated nanoclusters were observed in the cross-sectional images. Fig. 3(b) shows an enlarged HRTEM image of segregated particles. Note that the segregated particles do not necessarily nucleate

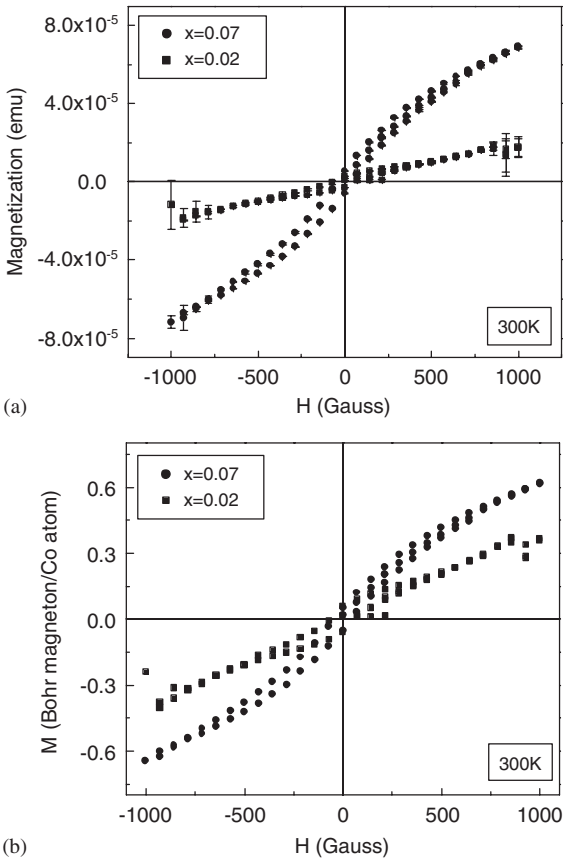

Fig. 1. An M–H curve for $Co_xTi_{1-x}O_2$ ($x = 0.07$, 0.02) thin films on $LaAlO_3$(0 0 1) taken at room temperature. Magnetic field was applied parallel to the film surface. (a) Magnetization (emu) vs. Magnetic field (H, G), (b) Magnetization(μ_B/Co atom) vs. Magnetic field (H, G).

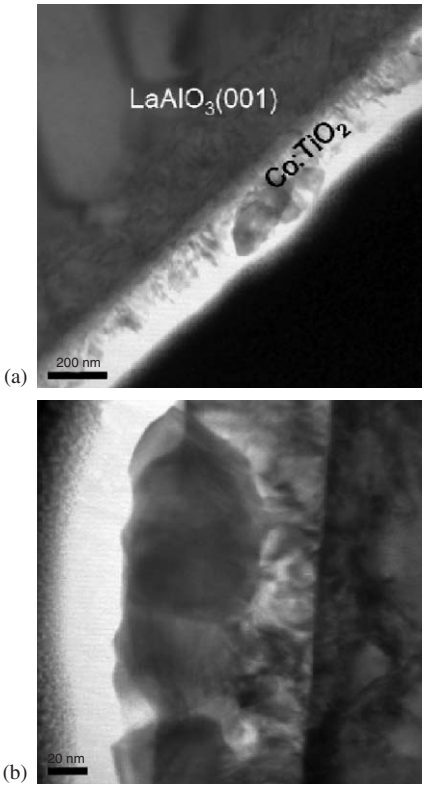

Fig. 2. A cross-sectional HRTEM image (a) and an enlarged image (b) taken from a $Co_{0.07}Ti_{0.93}O_2$ thin film.

at the substrate surface, but rather within the continuous anatase film. Similar nanoparticles have been reported for Co-doped TiO_2 films grown on $LaAlO_3$(0 0 1) by MBE [15]. Bright-field images and corresponding selected-area diffraction patterns (SADPs) for Co-doped TiO_2 films grown by reactive sputter deposition are shown in Figs. 3–5. The diffraction patterns are taken from the designated areas of the film cross-section. In particular, SADPs in Fig. 4 were taken from the $LaAlO_3$(0 0 1) substrate (region 1), (Co, Ti)O_2 thin film (region 2), and interface between $LaAlO_3$(0 0 1) substrate and (Co, Ti)O_2 thin films (region 3). The epitaxial relationship is seen to be (0 0 1)$LaAlO_3$ // (0 0 1)anatase and [0 0 1]$LaAlO_3$// [0 0 1]anatase. These results are consistent with four-circle XRD measurements taken on the same samples. Most interesting is the selected area electron diffraction patterns of the secondary particles. Fig. 5 shows a SADP taken from region 4 in Fig. 3(b) for the $Co_{0.07}Ti_{0.93}O_2$ thin film, corresponding to a segregated particle. The selected area electron diffraction pattern from the particle is consistent with the anatase crystal structure.

Note that, from the thermodynamic point of view, cobalt oxide is less stable than TiO_2 at low water vapor pressures for the growth temperatures considered.

Fig. 6 shows a HRTEM image taken from a segregated particle. Again the lattice spacing is consistent with the anatase phase. Local area EDS was performed on cross sections containing the secondary phase particles. The data shown in Fig. 7 acquired from each cluster confirms a large concentration of Co in these clusters. These segregated particles show a stronger Co signal than the area of TiO_2 film between the particles. In addition, as shown in Fig. 7, the intensity of the Ti peak decreases at the same position that the Co peak increases, indicating that these segregated nanoclusters contains Ti, and that the Ti signal is not simply intensity from adjacent regions. We also measured EDS on several different areas between the segregated particles.

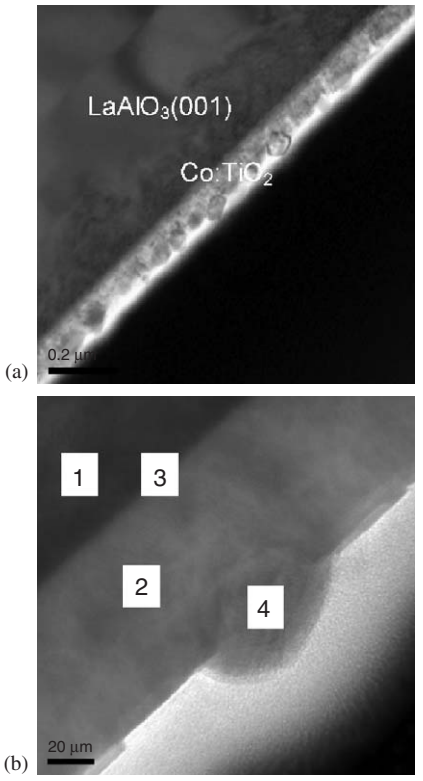

Fig. 3. A cross-sectional HRTEM image of a $Co_{0.07}Ti_{0.93}O_2$ thin films (a) and a magnified image for surface segregration of a $Co_{0.07}Ti_{0.93}O_2$ thin films (b): Region 1 ($LaAlO_3$(0 0 1) substrate), region 2 ((Co, Ti)O_2 thin film, region 3 (interface between $LaAlO_3$(0 0 1) substrate and (Co, Ti)O_2 thin films), region 4 (segregated particles on the surface of films).

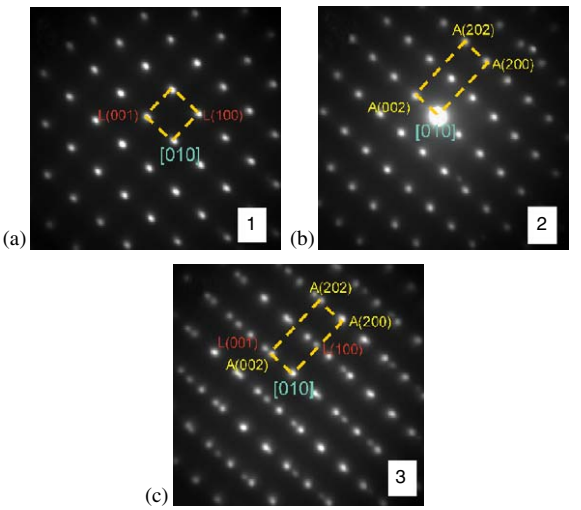

Fig. 4. Selected-area diffraction patterns (SADPs) taken from a $Co_{0.07}Ti_{0.93}O_2$ thin films in Fig. 3 for (a) region 1, (b) region 2 and (c) region 3.

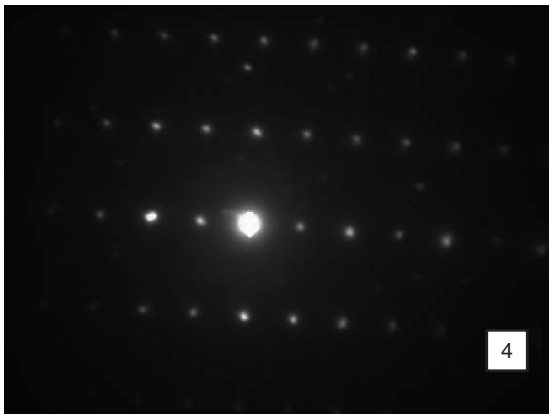

Fig. 5. Selected-area diffraction patterns (SADPs) taken from the secondary phase particle (region 4) in the $Co_{0.07}Ti_{0.93}O_2$ thin films in Fig. 3.

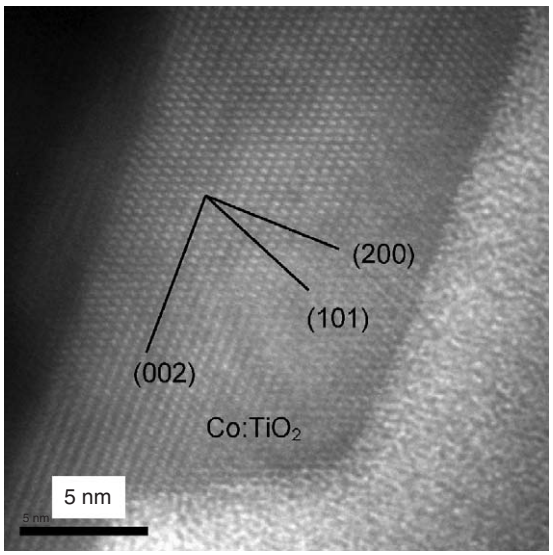

Fig. 6. A lattice image taken from a $Co_{0.07}Ti_{0.93}O_2$ thin film.

There were weak Co signals away from the clusters, indicating the presence of Co inside the TiO_2 film matrix. Fig. 8 shows chemical mapping data taken with EDS from $Co_{0.07}Ti_{0.93}O_2$ anatase thin films. Ti was roughly uniform throughout the entire cross-section area. The Co peak is clearly higher in intensity in the particle as compared to the remainder of the film. The oxygen peak was observed over the entire film area. While the segregation of Co into Co-rich TiO_2 precipitates is consistent with that observed in MBE-grown films, this is in contrast to work

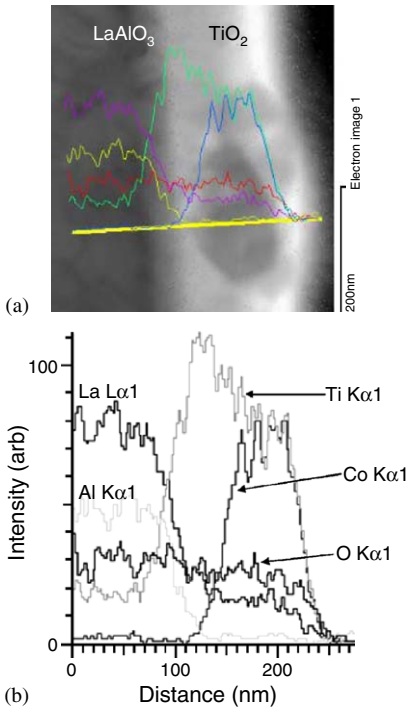

Fig. 7. HRTEM image taken from secondary phase particle and EDS data for $Co_{0.07}Ti_{0.93}O_2$ film.

reported for insulating films sputter deposited with Ar from a ceramic $(Ti,Co)O_2$ target [16]. The differences in segregated microstructure may originate from the use of water vapor as the oxidizing species, as well as the use of metal source targets. Both of these conditions would tend to yield oxygen-deficient films similar to those grown by MBE from metal sources.

In conclusion, the crystal structure and composition of segregated particles in Co-doped TiO_2 films grown by reactive sputter deposition were examined. The secondary particles are found to be Co-enriched TiO_2 anatase. EDS mapping, line scan and AES results show higher Co intensity on these particles than that of the rest of the films. Therefore, from these results and SADPs data, we confirm that the segregated particles observed on the surface of $Co_{0.07}Ti_{0.93}O_2$ thin films are Co-enriched anatase. Similar results have been reported for films grown by MBE at slow growth rates [12], in which highly Co-enriched anatase nanoclusters are observed on the surface of the

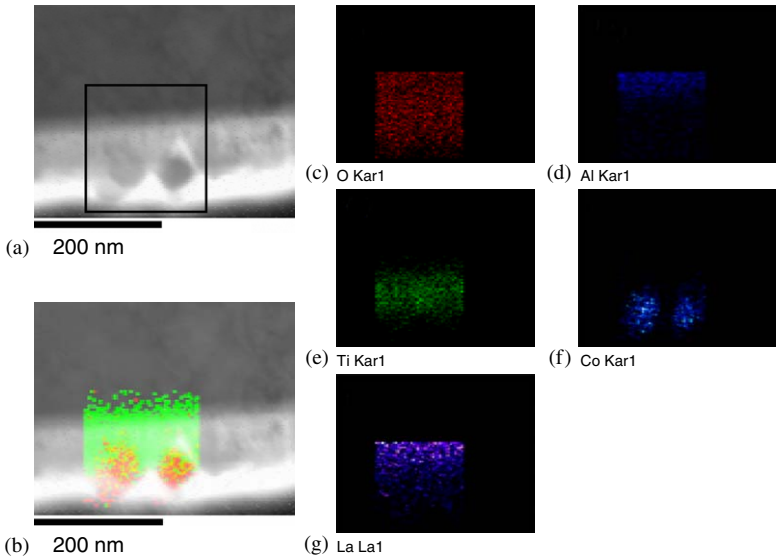

Fig. 8. EDS data for $Co_{0.07}Ti_{0.93}O_2$ film.

films. From our SADPs results, neither metallic Co nor Co oxide clusters are observed in the films.

Acknowledgments

This work was partially supported by the Army Research Office through research Grant DAAD 19-01-1-1508. The authors would also like to acknowledge the staff of the Major Analytical Instrumentation Center, Department of Materials Science and Engineering, University of Florida, for their assistance with this work.

References

[1] S. Datta, B. Das, Appl. Phys. Lett. 56 (1990) 665.
[2] S.A. Wolf, D.D. Awschalom, R.A. Buhrman, J.M. Daughton, S. Von Molnar, M.L. Roukes, A.Y. Chechelkanova, D.M. Treger, Science 294 (2001) 1488.
[3] D.D. Awschalom, M. E. Flatté, N. Samarth, Sci. Am. June (2002).
[4] Y.D. Park, A.T. Hanbicki, S.C. Erwin, C.S. Hellberg, J.M. Sullivan, J.E. Matson, T.F. Ambrose, A. Wilson, G. Spanos, B.T. Jonker, Science 295 (2002) 651.
[5] H. Ohno, F. Matskura, T. Omiya, N. Akiba, J. Appl. Phys. 85 (1999) 4277.
[6] H. Ohno, A. Shen, F. Matsukura, A. Oiwa, A. Endo, S. Katsumoto, Y. Iye, Appl. Phys. Lett. 69 (1996) 363.
[7] Y. Matsumoto, M. Murakami, T. Shono, T. Hasegawa, T. Fukumura, M. Kawasaki, P. Ahmet, T. Chikyow, S.-Y. Koshihara, H. Koinuma, Science 291 (2001) 854.
[8] D.H. Kim, J.S. Yang, K.W. Lee, S.D. Bu, T.W. Noh, S.-J. Oh, Y.-W. Kim, J.-S. Chung, H. Tanaka, H.Y. Lee, T. Kawai, Appl. Phys. Lett. 81 (2002) 2421.
[9] S.A. Chambers, S. Thevuthasan, R.F.C. Farrow, R.F. Marks, J.U. Thiele, L. Folks, M.G. Samant, A.J. Kellock, N. Ruzycki, D.L. Ederer, U. Diebold, Appl Phys. Lett. 79 (2001) 3457.
[10] S.A. Chambers, C.M. Wang, S. Thevuthasan, T. Droubay, D.E. McCready, A.S. Lea, V. Shutthanandan, C.F. Windisch Jr., Thin Solid Films 418 (2002) 197.
[11] S.R. Shinde, S.B. Ogale, S. Das Sarma, J.R. Simpson, H.D. Drew, S.E. Lofland, C. Lanci, J.P. Buban, N.D. Browning, V.N. Kulkarni, J. Higgins, R.P. Sharma, R.L. Greene, T. Venkatesan, Phys. Rev. B. 67 (2003) 115211.
[12] S.A. Chambers, T. Droubay, C.M. Wang, A.S. Lea, R.F.C. Farrow, L. Folks, V. Deline, S. Anders, Appl. Phys. Lett. 82 (2003) 1257.
[13] B.–S. Jeong, Y.W. Heo, D.P. Norton, J.G. Kelly, R. Rairigh, A.F. Hebard, J.D. Budai, Y.D. Park, Appl. Phys. Lett. 8 (2004) 2608.
[14] B.-S. Jeong, D.P. Norton, J.D. Budai, Solid-State Electron. 47 (2003) 2275.
[15] S.A. Chambers, R.F.C. Farrow, MRS Bull. 28 (2003) 729.
[16] K.A. Griffin, A.B. Pakhomov, C.M. Wang, S.M. Heald, K.M. Krishnan, Phys. Rev. Lett. 94 (2005) 157204.